Proc. Natl. Acad. Sci. USA
Vol. 83, pp. 2056–2060, April 1986
Biochemistry

A mutant of *Escherichia coli* fumarate reductase decoupled from electron transport

(iron–sulfur/flavin redox centers)

JOEL H. WEINER*†, RICHARD CAMMACK‡, STEWART T. COLE§, CARO CONDON*, NADINE HONORÉ§, BERNARD D. LEMIRE*, AND GILLIAN SHAW*

*Department of Biochemistry, University of Alberta, Edmonton, AB, T6G 2H7 Canada; ‡Department of Plant Sciences, Kings College, 68 Half Moon Lane, London, SE24 9JF England; and §Groupment de Génie Génétique, Institut Pasteur, 28 Rue du Dr. Roux, 75724 Paris 15, France

Communicated by Leon A. Heppel, November 25, 1985

ABSTRACT **The terminal electron-transfer enzyme fumarate reductase of *Escherichia coli* is a complex iron–sulfur flavoenzyme composed of four nonidentical subunits organized into two domains: FrdA and -B (a membrane-extrinsic catalytic domain) and FrdC and -D (a transmembrane anchor domain). We have identified a mutation within the membrane-intrinsic domain that alters the electron transfer properties of the iron–sulfur and flavin redox centers of the catalytic domain. Functional electron flow from the quinone analog 2,3-dimethyl-1,4-naphthoquinone or from the electron transport chain is impaired. However, the mutant enzyme can be reduced normally by single-electron donors such as the dye benzyl viologen. The mutant phenotype results from a single A → G transition changing His-82, within the second transmembrane α-helix of the FrdC anchor sequence, to an arginine. The mutation, physically located within the anchor domain, is manifested by altered catalytic properties, indicating that the intrinsic and extrinsic domains are conformationally connected. These results confirm the important role of the anchor subunits in functional electron transport and have implications for communication between intrinsic and extrinsic domains of membrane proteins.**

Fumarate reductase is a complex, membrane-bound iron–sulfur flavoenzyme that serves as the terminal electron-transfer enzyme when *Escherichia coli* is grown anaerobically with fumarate as the electron acceptor (1). The enzyme is composed of two distinct domains: a membrane-extrinsic catalytic domain comprised of the FrdA and -B polypeptides of 69 and 27 kDa, respectively, and a membrane-intrinsic domain consisting of the FrdC and -D subunits of 15 and 13 kDa, respectively (2). Two forms of the enzyme can be isolated: a tetrameric holoenzyme, composed of equimolar amounts of each subunit, and a catalytic dimer, composed of the FrdA and -B subunits (3, 4). By analogy with the *E. coli* succinate dehydrogenase, the active site of fumarate reductase is located in FrdA, the flavin-containing subunit (5). The iron–sulfur centers are located in the FrdB subunit (6) and the FrdC and -D polypeptides do not contain any known redox centers. The FrdC and -D polypeptides not only anchor the catalytic subunits to the membrane surface (4) but also induce an optimal conformation in the catalytic dimer as reflected by increased stability and modulated turnover of the holoenzyme (7). The enzyme is believed to accept reducing equivalents (electrons) from a reduced *b*-type cytochrome buried within the membrane. However, the pathways for electrons within the electron transport chain and within the enzyme itself remain to be firmly established.

The publication costs of this article were defrayed in part by page charge payment. This article must therefore be hereby marked "*advertisement*" in accordance with 18 U.S.C. §1734 solely to indicate this fact.

Previously characterized mutants of the *frd* operon have been localized to the *frdA* gene (8). We now report the isolation and analysis of a mutant within the FrdC subunit. Mutant enzyme is unable to accept electrons from either the physiological donor or the quinone analog 2,3-dimethyl-1,4-naphthoquinone (DMN) and yet functions normally with the artificial electron donor reduced benzyl viologen (BV_{red}). The differential utilization of electron donors indicates the presence of two spatially distinct sites at which reduction can occur.

MATERIALS AND METHODS

DMN was the gift of A. Kröger (Phillips University, Marburg, F.R.G.). Bacterial strains and plasmids are described in Table 1.

Growth of Cells and Preparation of Inverted Membrane Vesicles. All cells were grown at 37°C. For anaerobic growth, glucose/peptone, glycerol/fumarate, or glycerol/nitrate medium was prepared as described (9). For growth with H_2 (H_2/fumarate medium), the glycerol/fumarate medium was supplemented with 0.5% peptone and sparged with H_2/CO_2 (95:5). Flasks were filled to the top with medium and stoppered. Cells were inoculated at 1% (vol/vol) from an aerobic overnight culture on L-broth (10). Amino acids, vitamins, and ampicillin (100 μg/ml) were added as needed. Cultures were harvested after 24 hr. Membrane vesicles were prepared by French pressure lysis (Aminco) as described (4).

Isolation of Mutant GS19. A mid-log phase culture of *E. coli* HB101 grown on L-broth was mutagenized with *N*-methyl-*N'*-nitro-*N*-nitrosoguanidine (40 μg/ml) for 7.5 min at 37°C in 0.1 M citrate buffer, pH 5.5 (10). The cells were washed with 0.1 M potassium phosphate buffer (pH 7.0), resuspended in L-broth, grown overnight, and then transferred to GF medium for 36 hr of aerobic growth to eliminate auxotrophs. The culture was exposed to one cycle of ampicillin enrichment (100 μg/ml) in anaerobic glycerol/fumarate medium and subsequently plated on L-broth plates, from which single colonies were replicated to duplicate glycerol/fumarate plates and incubated either anaerobically or aerobically. Each mutant unable to grow anaerobically was transformed with plasmid pFRD84 (4) and ampicillin-resistant transformants were selected. Mutants complemented by pFRD84 were *frd* mutants. Cell-free extracts from the *frd* mutants were assayed for fumarate-dependent benzyl viologen oxidase activity.

Cloning of a Mutant *frd* Operon. Chromosomal DNA was digested with endonuclease *Hin*dIII, and fragments of about 4.9 kilobase pairs were purified by gel electrophoresis and NACS column chromatography (Bethesda Research Laboratories). Purified DNA was ligated into dephosphorylated,

Abbreviations: DMN, 2,3-dimethyl-1,4-naphthoquinone; $DMNH_2$, reduced DMN; BV_{red}, reduced benzyl viologen; HOQNO, 2-*n*-heptyl-4-hydroxyquinoline *N*-oxide.

†To whom correspondence should be addressed.

Table 1. Strains and plasmids

	Description	Vector	Source
E. coli strains			
HB101	F⁻, *hsdR, hsdM, pro, leu, lac, gal, thi, recA, rpsL*	—	G. McFadden*
GS1	*frdA4* mutant from HB101	—	Laboratory collection
GS19	*frdC1* mutant from HB101	—	This study
Plasmids			
pFRD84	Ap, $frdA^+B^+C^+D^+$	pBR322	Ref. 4
pFRD117	Ap, $frdA^+B^+$	pBR322	Ref. 4
pFRD215	Ap, $frdC^+D^+$	pBR322	See legend
pFRD704	Ap, $frdC^+$	pBR322	See legend
pFRD38	Ap, $frdD^+$	pUC8	G. Cecchini†
pFRD300	Ap, $frdA^+B^+C^-D^+$	pUC13	This study

pFRD215 was generated by restriction endonuclease *Sac* II digestion of pFRD84 followed by ligation with T4 DNA ligase (4). pFRD704 is a BAL-31 exonuclease-generated deletion of pFRD215 lacking all but the first 36 nucleotides of *frdD* coding sequence.

*University of Alberta.

†University of California, San Francisco.

*Hin*dIII-cut pUC13 vector DNA (Pharmacia P-L Biochemicals) and used to transform competent GS1 ($frdA^-$) cells. Ampicillin-resistant transformants were selected and tested for growth on glycerol/fumarate plates incubated anaerobically. A few poorly growing colonies were detected and small-scale preparations of their plasmid DNA were screened (11). pFRD300 contained the mutant fumarate reductase operon on the expected *Hin*dIII fragment (12).

DNA Sequence Analysis. This was performed as described (13) except that in some reaction mixtures GTP was replaced by ITP.

Fumarate Reductase Assays. The BV_{red} assay was as described (3, 14). The reduced DMN ($DMNH_2$) assay was a modification of the method of Kröger and Innerhofer (15). Assays were performed in a final volume of 1.1 ml of N_2-saturated 50 mM potassium phosphate (pH 8.0). The assay contained 0.5 mM DMN and 1 mM fumarate. Reduction of DMN was accomplished by the addition of 2 mM $NaBH_4$. The reaction was started by the addition of 5–20 units of fumarate reductase (BV_{red} oxidase activity) and the increase in absorption at 270 nm was followed. One unit corresponds to 1 μmol of $DMNH_2$ oxidized per min at 24°C. The extinction coefficient of DMN at 270 nm is 16,000 M^{-1} (15).

Quinacrine Fluorescence Quenching. Assays were performed as described (16), using either H_2- or N_2-saturated buffers. The reaction was initiated with 0.5 μmol of fumarate. 2-*n*-Heptyl-4-hydroxyquinoline *N*-oxide (HOQNO) was used at 6 μM.

Protein Determination. Protein was estimated by a modified Lowry procedure (17).

Limited Proteolysis Analysis. *Staphylococcus aureus* V8 protease digestion was performed on gel slices as described (18). Digests were run on $NaDodSO_4$/15% polyacrylamide slab gels with low molecular weight protein standards (Bethesda Research Laboratories). Gels were scanned on a Joyce–Loebl Chromoscan 3 densitometer. V8 protease was the gift of L. B. Smillie (University of Alberta, Edmonton, Canada).

EPR Spectroscopy. EPR spectra were recorded on a Varian E4 spectrometer fitted with an E1020 microwave bridge and an Oxford Instruments ESR9 liquid helium flow cryostat. Samples were analyzed in cylindrical quartz cuvettes of 3.5 mm internal diameter.

RESULTS

Characterization of Mutant GS19. Mutagenesis of *E. coli* HB101 was performed to isolate fumarate reductase mutants. Mutant GS19 was unique in that, although unable to grow anaerobically on glycerol with fumarate as electron acceptor, it had normal fumarate-dependent BV_{red} oxidase activity. The mutant grew anaerobically on glycerol/nitrate, glucose/peptone, and, surprisingly, on H_2/fumarate media, indicating that it was not defective in an essential electron transport component (Table 2). Measurements of the menaquinone, ubiquinone, and *b*-type cytochrome levels confirmed that these components were present in normal amounts (data not shown).

Complementation Studies. Plasmids carrying all or part of the wild-type *frd* operon were transformed into GS19 and anaerobic growth on glycerol/fumarate medium was assayed. pFRD84, carrying a complete *frd* operon, could complement the mutation (Table 2). Both pFRD117, which expresses the FrdA and -B polypeptides, and pFRD215, which produces the FrdC and -D subunits, could complement (Table 2). Further, pFRD704, which carries *frdC* alone, could complement, whereas pFRD38 bearing *frdD* could not.

Limited Proteolysis. Fumarate reductase polypeptides from the mutant (pFRD300) and wild-type (pFRD84) enzyme were compared by limited proteolysis with V8 protease. The peptide profiles obtained for each of the two FrdC/D patterns

Table 2. Growth studies on anaerobic medium

Medium	Strain	Klett units
Glycerol/fumarate	HB101	64
	GS19	3
	GS19/pFRD84	109
	GS19/pFRD117	100
	GS19/pFRD215	95
	GS19/pFRD704	105
	GS19/pFRD38	10
	HB101/pFRD84	88
	HB101/pFRD300	15
Glycerol/nitrate	HB101	118
	GS19	91
	HB101/pFRD84	88
	HB101/pFRD300	142
Hydrogen/fumarate	HB101	202
	GS19	165

All growth experiments were performed at 37°C. Cultures were inoculated with a 1% (vol/vol) inoculum of an overnight aerobic L-broth culture into 125-ml Klett flasks filled to the top and were stirred slowly on a magnetic stirrer. When hydrogen was used, the flasks were continuously sparged with filtered gas through a serum cap. After 24 hr of growth, readings were taken in a Klett colorimeter using a red filter. Expression of *frdD* on plasmid pFRD38 was under tryptophan control and was induced with indole-3-acetic acid (10 μg/ml).

(the anchor polypeptides were not resolved in this system) show several differences, of which the most striking is a novel peptide in the mutant sample (Fig. 1). The fumarate reductase proteins are relatively resistant to digestion by V8, and the protease was employed at relatively high concentration (see legend to Fig. 1). Under these conditions V8 protease can cleave after histidine, in addition to normal cleavage after glutamate (19).

Cloning and Sequence Analysis. To determine the exact nature of the mutation in GS19, the mutant *frd* operon was cloned in pUC13, generating plasmid pFRD300. The genetic properties of pFRD300 resembled those of GS19 except that a partial diploid exhibited a negative-dominance phenotype when grown on glycerol/fumarate medium (Table 2). To resolve the discrepancy in the complementation experiments and to localize the mutation, we determined the DNA sequences of *frdA*, *-B*, and *-C* and compared them to those of the wild type (6, 13, 20). A single base difference was observed, an A → G transition at position 3575. This changes His-82 in the second transmembrane α-helix of the FrdC polypeptide to arginine.

Catalytic Properties of the Mutant Enzyme. The BV_{red} oxidase activity of fumarate reductase in lysates of GS19 is comparable to that of the parental strain (Table 3). Further, the enzyme levels of cells harboring either the cloned wild-type or the mutant operons are similar. In the BV_{red} assay, the K_m for fumarate was the same for both enzymes (425 μM). However, the specific activity of purified mutant holoenzyme was 3.5-fold higher than that of wild-type holoenzyme (550 units/mg vs. 150 units/mg) and approached the high specific activity of catalytic dimer (13). Kröger and Innerhofer (15) have shown that the quinone analogue $DMNH_2$ can serve as a donor of reducing equivalents to fumarate reductase of *Wollinella succinogenes* in the presence of the *b*-type cytochrome subunit. We assayed $DMNH_2$ oxidase activity to characterize fumarate reductase of *E. coli* and found that this activity is retained upon solubilization and purification of holoenzyme but is completely absent when the FrdC and -D subunits are removed during purification of the catalytic dimer. The $DMNH_2$ oxidase activity of membrane-bound or purified wild-type holoenzyme is inhibited by HOQNO, whereas the BV_{red} oxidase activity is resistant (Table 3). The mutant enzyme possesses a greatly diminished $DMNH_2$ oxidase activity. Thus, with respect to turnover number and $DMNH_2$ activity, the mutant holoenzyme resembles isolated catalytic dimer.

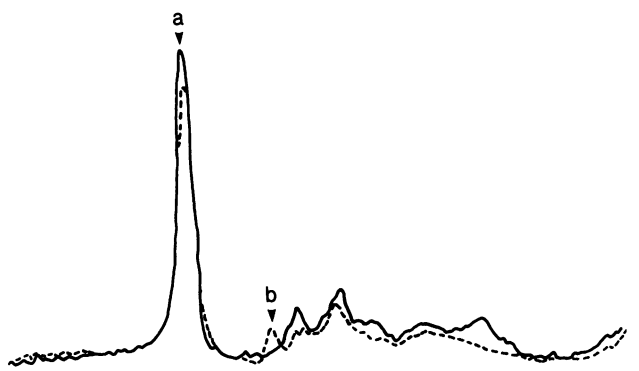

FIG. 1. Limited proteolysis of wild-type and mutant fumarate reductase polypeptides C and D. Excised FrdC/D polypeptide band from electrophoresis of 60 μg of purified tetramer was treated with 0.5 μg of *S. aureus* V8 protease and analyzed by $NaDodSO_4$/15% PAGE. Densitometric scans of lanes from a Coomassie blue-stained gel are shown. Solid line, pFRD84; dashed line, pFRD300. Undigested C/D protein at ≈15 kDa (a) and the novel peptide in mutant C/D profile at 10 kDa (b) are indicated.

Table 3. Fumarate reductase activity of membranes and extracts

Strain	BV_{red} activity		$DMNH_2$ activity	
	− HOQNO	+ HOQNO	− HOQNO	+ HOQNO
	Membrane-bound			
HB101	3.6	3.5	ND	ND
GS19	3.7	3.6	ND	ND
HB101/pFRD84	28.3	28.9	0.424	0.026
HB101/pFRD300	48.6	44.7	0.024	0.008
	Detergent-extracted			
HB101	4.9	4.9	0.042	0.008
GS19	8.7	8.8	ND	ND
HB101/pFRD84	37.9	39.6	0.502	0.029
HB101/pFRD300	93.0	91.2	0.030	0.006

Activities are reported as μmol of BV_{red} or $DMNH_2$ oxidized per min per mg of protein. Membrane-bound activity was measured using vesicles obtained by French pressure lysis. Detergent-extracted enzyme was prepared by 1% octaethyleneglycol mono(*n*-dodecyl) ether ($C_{12}E_8$, Nikkol Chemicals, Tokyo) extraction exactly as reported for Triton X-100 (4). HOQNO was used at 6 μM. ND, not determined.

Physical Properties of the Mutant Enzyme. Chromosomal or plasmid-encoded mutant fumarate reductase is membrane-bound and not released by salt or EDTA washes (data not shown). This indicates that the mutation in *frdC*, which encodes one of the anchor subunits, does not alter membrane association of the catalytic dimer. The subunit molecular weights and stoichiometry are identical to those of the wild type. The isoelectric points and the V8 protease digestion patterns of FrdA and -B of the mutant holoenzyme (data not shown) were similar to those of FrdA and -B of the wild-type holoenzyme (2).

Electron Transfer Properties. The greatly diminished ability of the mutant enzyme to oxidize $DMNH_2$ suggested that the mutation decoupled fumarate reductase from the electron transport chain. This decoupling is manifested as an impaired fumarate-dependent protonmotive force formation, as measured by quinacrine-fluorescence quenching. Inverted mutant membrane vesicles incubated with glycerol-3-phosphate do not exhibit fumarate-dependent quinacrine quenching (data not shown). Membrane vesicles from HB101 substantially quench quinacrine fluorescence in a H_2- and fumarate-dependent, HOQNO-sensitive manner (Fig. 2). In contrast, GS19 membranes exhibit much less quenching, and this quenching is HOQNO-resistant. In fact, the presence of HOQNO amplifies the quenching, suggesting that the inhibitor blocks proton-leakage pathways in the mutant membranes. We attribute the quenching observed with mutant membranes to the vectorial mechanism of hydrogenase and not to the vectorial action of the electron transport chain (21). That fumarate-dependent oxidation of NADH or dihydroorotate (22) is totally absent in the mutant membranes (data not shown) supports this.

EPR Properties. French press membrane vesicles and fumarate reductase tetramer from both mutant and wild-type cells were examined by EPR spectroscopy. The mutant enzyme exhibited all the features previously described for the iron–sulfur centers of wild-type fumarate reductase (23, 24). In the oxidized state (Fig. 3, spectrum a), it displayed a signal at $g = 2.02$ due to center 3, which is probably a [3Fe–*x*S] cluster. On reduction with succinate or brief treatment (1 min) with 2 mM dithionite, an axial spectrum at $g = 2.03, 1.93$ was observed, due to the [2Fe–2S] center 1. On further incubation with 2 mM dithionite, an additional reduction of the enzyme took place which was observed as an increase in the spin-lattice relaxation rate of the $g = 1.93$ signal. This reduction is attributed to center 2, which, from the amino acid sequence, is likely to be a [4Fe–4S] cluster. In our experi-

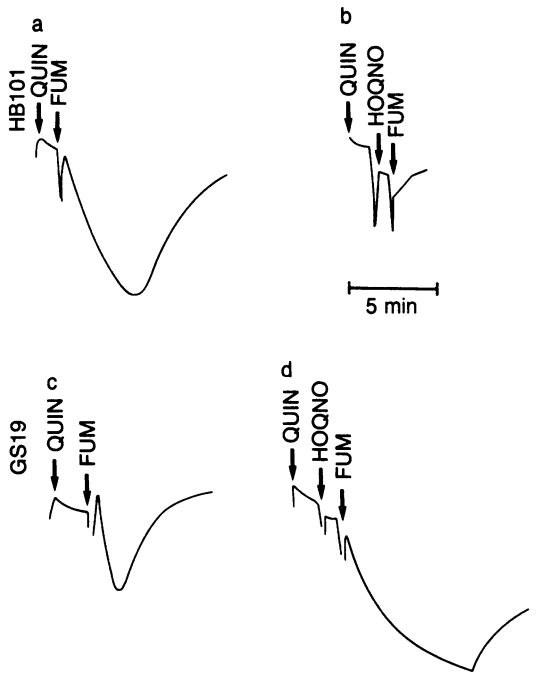

FIG. 2. Quinacrine-fluorescence quenching. (*a*) Membrane vesicles (1.62 mg of protein in 2.5 ml of assay buffer) prepared from *E. coli* HB101 by French pressure lysis were saturated with H_2 for 18 min prior to assay. Quinacrine (10 μmol) and fumarate (0.5 μmol) were added at the indicated times. (*b*) As in *a* except that 6 μM HOQNO was added. (*c*) As in *a* except that vesicles were prepared from *E. coli* GS19. (*d*) As in *b* except that vesicles were prepared from GS19.

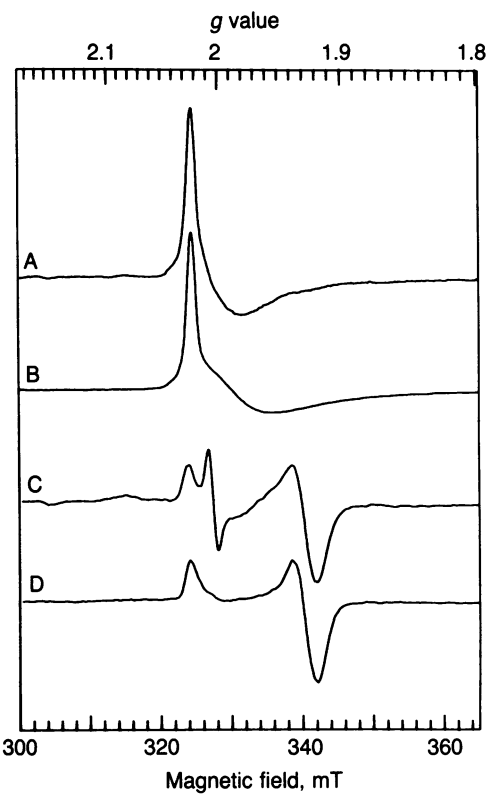

FIG. 3. EPR spectra of fumarate reductase in French press membrane vesicles from *E. coli* mutant HB101/pFRD300 (spectra a and c) and wild-type HB101/pFRD84 (spectra b and d). Spectra a and b: oxidized state, showing the signal of center 3 at $g = 2.02$. Spectra c and d: reduced with 5 mM dithionite at 20°C for 2 min; the signals of center 1 at $g = 2.03$ and 1.93 are seen. Spectrum c also shows the signal of a flavin radical at $g = 2.004$. Spectra were recorded at 11K; microwave power was 2 mW for spectra a and b and was 2 μW for spectra c and d.

ments, the reduction of center 2 does not contribute significantly to the intensity of the $g = 2.03$, 1.93 signal but corresponds to the appearance of an extremely broad signal centered around $g = 1.95$ (23, 25). A broad signal, of somewhat different lineshape, was also observed during reduction of center 2 in membranes of the mutant.

Although the EPR spectra observed with the mutant enzyme were qualitatively similar to those observed with the wild-type enzyme, there were differences observed during the time-course of reduction by dithionite. First, a flavin-radical signal was more intense in the mutant enzyme (Fig. 3, spectrum c) and remained for several minutes before it disappeared as a result of further reduction. Second, the reduction of center 1 was unusually slow, requiring 10 min for completion. This suggests that the normal pathway for reduction of the fumarate reductase by dithionite is absent in the mutant.

DISCUSSION

Fumarate reductase, a complex iron–sulfur flavoenzyme, contains at least three prosthetic groups capable of undergoing oxidation–reduction reactions (1, 2). These include two or three iron–sulfur centers, likely located in the FrdB subunit (6), and a covalent flavin cofactor in the FrdA subunit (26). Here, we report the isolation and characterization of an unusual mutation that decouples fumarate reductase from the electron transport chain and prevents anaerobic growth of *E. coli* on glycerol/fumarate medium. The mutation is a single A → G transition in *frdC* that changes His-82, within a proposed transmembrane α-helix, to arginine. In a model for the topography of the anchor subunits (2), this histidine residue is located close to the cytoplasmic surface of the membrane and could be expected to interact with the catalytic subunits.

The properties of the mutant fumarate reductase suggest the presence of two distinct sites at which reduction of the enzyme can occur (Fig. 4). The electron transport chain normally carries electrons from hydrogenase or the primary dehydrogenases to fumarate reductase in a cytochrome-dependent manner. We suggest that the physiological donor and $DMNH_2$ use the same site to reduce the enzyme. This site is sensitive to HOQNO and requires the presence of the FrdC and -D subunits. Reducing equivalents are subsequently translocated within the enzyme to the iron–sulfur centers and the flavin. The second pathway for reducing equivalents is represented by the BV_{red} reaction site. This site can receive electrons from cytochrome-independent sources, is HOQNO-resistant, and does not require the FrdC and -D polypeptides. This pathway explains the cytochrome-independent electron transport from glycerol-3-phosphate to fumarate observed by Singh and Bragg in a heme-deficient mutant (27), the HOQNO-resistant protonmotive force observed by fluorescence quenching with H_2(g) in GS19 membranes, and the ability of this mutant to grow with H_2 and fumarate and may also explain the complementation of GS19 by pFRD117. The mutant enzyme is unable to oxidize $DMNH_2$ efficiently, although it uses BV_{red} normally. This suggests that the block precedes the site of BV_{red} oxidation.

Despite the absence of known redox groups in the FrdC and -D subunits, these polypeptides are essential for coupling the enzyme to the electron transport chain, or for receiving electrons from $DMNH_2$. Cecchini *et al.* (28) have observed that fumarate reductase, functioning as a succinate dehydrogenase, will reduce the quinone analog 2,3-dimethoxy-5-methyl-6-pentyl-1,4-benzoquinone only when the FrdC and

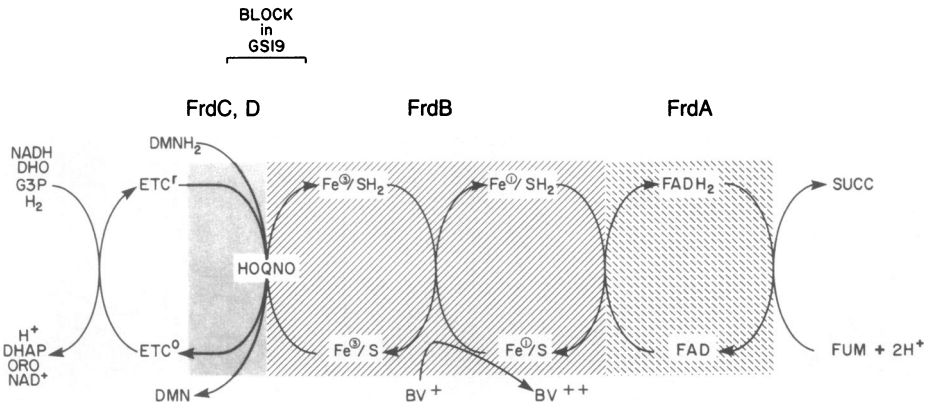

FIG. 4. A model for electron transport within fumarate reductase. Several primary dehydrogenases specific for NADH, dihydroorotate (DHO), glycerol-3-phosphate (G3P), and hydrogen couple to fumarate reductase via the electron transport chain. ETC^o and ETC^r refer to the oxidized and reduced components, respectively. $DMNH_2$ apparently also couples to this site. At least two iron–sulfur centers transfer electrons within FrdB. In this model, center 3 precedes center 1 [deduced from electrochemical potentials (23)]. The exact site of the BV_{red} (BV^+) reaction is unknown but it must precede at least one iron–sulfur center because the reaction is inhibited by *p*-chloromercuribenzenesulfonate (B.D.L. and J.H.W., unpublished observation). The apparent site of the block in GS19 is marked. ORO, orotate; DHAP, dihydroxyacetone phosphate; SUCC, succinate; FUM, fumarate.

-D subunits are present, substantiating the role of the anchor polypeptides in electron flow. These data support our conclusion that the C and D polypeptides are intimately involved in the redox reactions of fumarate reductase, in addition to their physical role as anchor subunits.

Two unexpected aspects of this work should be noted. First, although the mutation is in the *frdC* gene, a multicopy plasmid carrying *frdAB* could complement the mutation. We suggest that a large excess of soluble catalytic dimer from the plasmid pFRD117 can overcome the mutant phenotype by providing an accessible electron sink.

Second, cells harboring pFRD300 are unable to grow anaerobically on glycerol/fumarate medium, even though the chromosomal operon is normal. The negative-dominance effect is related to plasmid copy number (B.D.L. and J.H.W., unpublished data). Apparently, excess aberrant enzyme is capable of interfering with the normal flow of electrons from the dehydrogenase to the wild-type, chromosomally encoded fumarate reductase. Both of these results highlight the dangers of doing genetic experiments with multicopy plasmids.

The mutation within the FrdC polypeptide is reflected in changes to the redox properties of the iron–sulfur and flavin cofactors located in the catalytic domain. The reduction of iron–sulfur center 1 is slowed and the enzyme displays an unusually stable flavin semiquinone. Thus, the mutation is phenotypically transmitted from the membrane-intrinsic anchor subunits to the extrinsic catalytic subunits. The high specific activity of the mutant holoenzyme with BV_{red} as electron donor resembles that of the isolated catalytic dimer and suggests that the anchors regulate the turnover of the enzyme. We cannot yet distinguish whether the anchors actively participate in electron transport or induce a conformation within catalytic dimer necessary for physiological electron transport. The transmission of conformational changes from intrinsic to extrinsic subunits may operate in other membrane-bound enzymes and may explain the phenotype of several F_0/F_1 ATPase mutants (29).

This work was funded by the Medical Research Council of Canada (Grant MT5838 to J.H.W.) and by the Fondation Institut Pasteur (grant to S.T.C.). C.C. and B.D.L. received support from the Alberta Heritage Foundation for Medical Research.

1. Ingledew, W. J. & Poole, R. K. (1984) *Microbiol. Rev.* **48,** 222–271.
2. Weiner, J. H., Lemire, B. D., Jones, R. W., Anderson, W. F. & Scraba, D. G. (1984) *J. Cell. Biochem.* **24,** 207–216.
3. Dickie, P. & Weiner, J. H. (1979) *Can. J. Biochem.* **57,** 813–821.
4. Lemire, B. D., Robinson, J. J. & Weiner, J. H. (1982) *J. Bacteriol.* **152,** 1126–1131.
5. Wood, D., Darlison, M. G., Wilde, R. J. & Guest, J. R. (1984) *Biochem. J.* **222,** 519–534.
6. Cole, S. T., Grundström, T., Jaurin, B., Robinson, J. J. & Weiner, J. H. (1982) *Eur. J. Biochem.* **126,** 211–216.
7. Weiner, J. H., Elmes, M. L., Latour, D. J. & Lemire, B. D. (1984) *ICSU Rep.* **3,** 13–14.
8. Lambden, P. R. & Guest, J. R. (1976) *J. Gen. Microbiol.* **97,** 145–160.
9. Weiner, J. H., Lemire, B. D., Elmes, M. L., Bradley, R. D. & Scraba, D. G. (1984) *J. Bacteriol.* **158,** 590–596.
10. Miller, J. H. (1972) *Experiments in Molecular Genetics* (Cold Spring Harbor Laboratory, Cold Spring Harbor, NY), pp. 431–435.
11. Birnboim, H. C. & Doly, J. (1979) *Nucleic Acids Res.* **7,** 1513–1523.
12. Lohmeier, E., Hagen, D. S., Dickie, P. & Weiner, J. H. (1981) *Can. J. Biochem.* **59,** 158–164.
13. Cole, S. T. (1982) *Eur. J. Biochem.* **122,** 479–484.
14. Robinson, J. J. & Weiner, J. H. (1982) *Can. J. Biochem.* **60,** 811–816.
15. Kröger, A. & Innerhofer, A. (1976) *Eur. J. Biochem.* **69,** 497–506.
16. Jones, R. W. (1979) *Biochem. Soc. Trans.* **7,** 1135–1136.
17. Markwell, M. A. K., Haas, S. M., Bieber, L. L. & Tolbert, N. E. (1978) *Anal. Biochem.* **87,** 300–305.
18. Cleveland, D. W., Fischer, S. G., Kirschner, M. W. & Laemmli, U. K. (1977) *J. Biol. Chem.* **252,** 1102–1106.
19. Lau, Y. M. S., Sanders, C. & Smillie, L. B. (1985) *J. Biol. Chem.* **260,** 7257–7263.
20. Grundström, T. & Jaurin, B. (1982) *Proc. Natl. Acad. Sci. USA* **79,** 1111–1115.
21. Jones, R. W. (1980) *Biochem. J.* **188,** 345–350.
22. Newton, N. A., Cox, G. B. & Gibson, F. (1971) *Biochim. Biophys. Acta* **244,** 155–166.
23. Cammack, R., Patil, D. S., Condon, C., Owen, P., Cole, S. T. & Weiner, J. H. (1985) in *Flavins and Flavoproteins*, eds. Bray, R. C., Engel, P. C. & Mayhew, S. G. (de Gruyter, Berlin), pp. 551–554.
24. Simpkin, D. & Ingledew, W. J. (1985) *Biochem. Soc. Trans.* **13,** 602–607.
25. Cammack, R., Patil, D. S. & Weiner, J. H. (1986) *Biochim. Biophys. Acta*, in press.
26. Weiner, J. H. & Dickie, P. (1979) *J. Biol. Chem.* **254,** 8590–8593.
27. Singh, A. P. & Bragg, P. D. (1976) *Biochim. Biophys. Acta* **423,** 450–461.
28. Cecchini, G., Ackrell, B. A. C., Gunsalus, R. P. & Kearney, E. P. (1984) *ICSU Rep.* **3,** 575–576.
29. Futai, M. & Kanazawa, H. (1983) *Microbiol. Rev.* **47,** 285–312.